

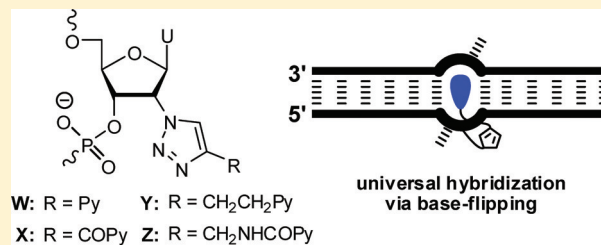
# C2'-Pyrene-Functionalized Triazole-Linked DNA: Universal DNA/RNA Hybridization Probes

Sujay P. Sau and Patrick J. Hrdlicka\*

Department of Chemistry, University of Idaho, Moscow, Idaho 83844, United States

**S** Supporting Information

**ABSTRACT:** Development of universal hybridization probes, that is, oligonucleotides displaying identical affinity toward matched and mismatched DNA/RNA targets, has been a longstanding goal due to potential applications as degenerate PCR primers and microarray probes. The classic approach toward this end has been the use of “universal bases” that either are based on hydrogen-bonding purine derivatives or aromatic base analogues without hydrogen-bonding capabilities. However, development of probes that result in truly universal hybridization without compromising duplex thermostability has proven challenging. Here we have used the “click reaction” to synthesize four C2'-pyrene-functionalized triazole-linked 2'-deoxyuridine phosphoramidites. We demonstrate that oligodeoxyribonucleotides modified with the corresponding monomers display (a) minimally decreased thermal affinity toward DNA/RNA complements relative to reference strands, (b) highly robust universal hybridization characteristics (average differences in thermal denaturation temperatures of matched vs mismatched duplexes involving monomer **W** are <1.7 °C), and (c) exceptional affinity toward DNA targets containing abasic sites opposite of the modification site ( $\Delta T_m$  up to +25 °C). The latter observation, along with results from absorption and fluorescence spectroscopy, suggests that the pyrene moiety is intercalating into the duplex whereby the opposing nucleotide is pushed into an extrahelical position. These properties render C2'-pyrene-functionalized triazole-linked DNA as promising universal hybridization probes for applications in nucleic acid chemistry and biotechnology.



## INTRODUCTION

The Cu<sup>I</sup>-catalyzed [3 + 2] azide–alkyne cycloaddition (CuAAC) reaction, which results in the formation of 1,4-disubstituted 1,2,3-triazoles,<sup>1,2</sup> has been extensively utilized for the synthesis of modified nucleosides, nucleotides, and oligonucleotides.<sup>3,4</sup> The remarkable progress over the past five years has paved the way for empowering applications in nucleic acid chemistry<sup>5</sup> such as postsynthetic labeling of oligonucleotides with reporter groups,<sup>6</sup> controlled metallization of oligonucleotides,<sup>7</sup> ligation of oligonucleotides,<sup>8,9</sup> and generation of oligonucleotides with artificial backbone<sup>10</sup> and nucleobase<sup>11,12</sup> motifs.

Our interest in (a) employing the CuAAC reaction within oligonucleotide chemistry,<sup>13</sup> (b) studying pyrene-functionalized oligonucleotide probes for potential diagnostic applications,<sup>13–17</sup> and (c) developing oligonucleotides modified with 2'-intercalator-functionalized nucleotide monomers for DNA-targeting applications<sup>18–21</sup> prompted us to explore oligodeoxyribonucleotides (ONs) that are modified with C2'-pyrene-functionalized triazole-linked 2'-deoxyuridine monomers **W–Z** (Figure 1). We surmised that the corresponding phosphoramidites would be readily available via CuAAC reactions using simple reagents and starting materials, and that the pyrene moieties of monomer **W–Z** intercalate into duplex cores as observed with O2'-intercalator-functionalized RNA,<sup>21–23</sup> N2'-intercalator-functionalized 2'-N-methyl-2'-amino-DNA,<sup>21,24</sup> and N2'-intercalator-functionalized 2'-amino- $\alpha$ -L-LNA.<sup>18–20</sup> Monomers **W–Z**

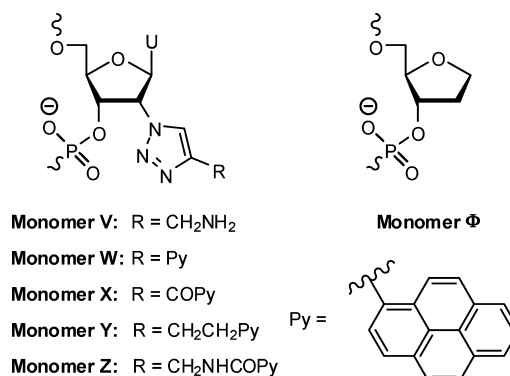


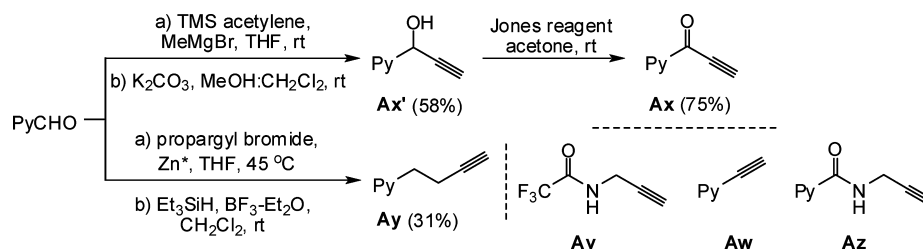
**Figure 1.** Structures of C2'-pyrene-functionalized triazole-linked 2'-deoxyuridine monomers and other monomers studied herein.

were specifically selected to study the influence of the linker between the pyrene and triazole moieties on hybridization properties of correspondingly modified ONs, while non-functionalized monomer **V** provides insight into the relative roles of pyrene and triazole moieties. Recent reports have described pre-<sup>25,26</sup> and postsynthetic<sup>6e,27</sup> uses of the CuAAC reaction for 2'-functionalization of nucleotides. To the best of our knowledge, the present work is the first example of

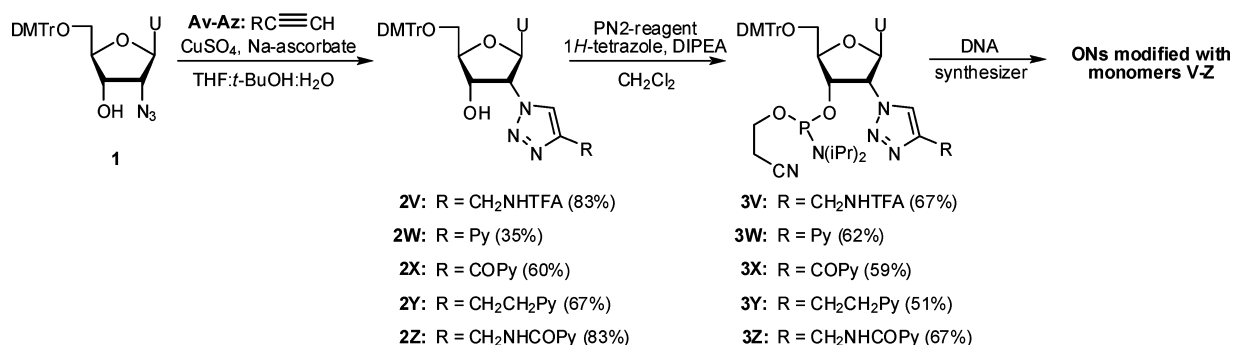
**Received:** September 7, 2011

**Published:** November 16, 2011

Scheme 1. Synthesis and Structures of Terminal Alkynes



Scheme 2. Synthesis of C2'-Pyrene-Functionalized Triazole-Linked Uridine Phosphoramidites 3V–3Z



ONs modified with monomers where pyrene-functionalized 1,2,3-triazolyl moieties are directly attached to the 2'-position of nucleosides.

Here we demonstrate that ONs modified with C2'-pyrene-functionalized triazole-linked monomers are robust universal DNA/RNA hybridization probes; that is, they display virtually identical DNA/RNA target affinity regardless of the nucleotide opposite of the modification site. Development of universal hybridization probes has been a longstanding goal due to their potential as degenerate PCR primers and microarray probes when the identity of one or more nucleotides in a target sequence is unknown.<sup>28–31</sup> The classic approach toward this end has been the use of ONs containing “universal bases”,<sup>32</sup> which fall into two categories: (a) aromatic base analogues without hydrogen-bonding capabilities such as 3-nitropyrrole,<sup>29</sup> 5-nitroindole,<sup>33</sup> isocarboxystyryl,<sup>34</sup> or pyrene,<sup>13,35–38</sup> and (b) hydrogen-bonding universal bases based on inosine<sup>39–41</sup> or other purine moieties.<sup>42,43</sup> However, development of truly “universal” hybridization probes that do not compromise duplex thermostability has proven challenging.<sup>44</sup>

## RESULTS AND DISCUSSION

**Phosphoramidite Synthesis.** 5'-O-Dimethoxytrityl-2'-azido-2'-deoxyuridine **1**<sup>45</sup> was identified as a suitable starting material for the synthesis of the target compounds. 2,2,2-Trifluoro-*N*-(prop-2-ynyl)acetamide **Av**,<sup>46</sup> 1-ethynylpyrene **Aw**,<sup>47</sup> and *N*-(prop-2-ynyl)pyrene-1-carboxamide **Az**<sup>48</sup> were prepared as previously described, while 1-(pyren-1-yl)-prop-2-yn-1-one **Ax** and 4-(pyren-1-yl)-but-1-yne **Ay** were obtained via novel routes (Scheme 1). Thus, nucleophilic addition of Me<sub>3</sub>SiC≡CMgBr (generated in situ from trimethylsilylacetylene and MeMgBr in THF) to pyrene-1-carboxaldehyde followed by desilylation using potassium carbonate provided **Ax'** in 58% yield. A subsequent Jones oxidation afforded **Ax** in 75% yield. Similarly, nucleophilic addition of HC≡CCH<sub>2</sub>ZnBr (generated in situ from propargyl bromide and activated zinc in THF) to pyrene-1-carboxaldehyde, followed by deoxygenation

of the resultant homopropargyl alcohol using trifluoroboron etherate and triethylsilane, afforded **Ay** in 31% yield.

Room temperature CuAAC reactions between **1** and terminal alkynes **Av–Az** provided the corresponding triazoles **2V–2Z** in robust yields (60–83%), except when using 1-ethynylpyrene **Aw**, which required heating (75 °C) to afford nucleoside **2W** in 35% yield (Scheme 2). Nucleosides **2V–2Z** were subsequently converted into phosphoramidites **3V–3Z** (51–67% yield) using 2-cyanoethyl-*N,N,N',N'*-tetraisopropylphosphordiamidite (PN2 reagent) and 1*H*-tetrazole as an activator. Alternative phosphorylation conditions were not investigated as the described route provided sufficient quantities of **3V–3Z** for further analysis.

**ON Synthesis and Experimental Design.** Phosphoramidites **3V–3Z** were incorporated into ONs via machine-assisted solid-phase DNA synthesis (0.2 μmol scale) using the following conditions (activator, coupling time, stepwise coupling yield): **3V** (4,5-dicyanoimidazole, 15 min, ~80%), **3W** (5-(ethylthio)-1*H*-tetrazole, 30 min, ~90%), **3X** (5-(bis-3,5-trifluoromethylphenyl)-1*H*-tetrazole [Activator 42]; 30 min, ~80%), **3Y** and **3Z** (4,5-dicyanoimidazole, 30 min, ~90%). Acceptable but non-optimized conditions (≥80% coupling yield) were identified through progressive screening of activators (4,5-dicyanoimidazole → 5-(ethylthio)-1*H*-tetrazole → Activator 42). After workup and HPLC purification, the composition and purity of all modified ONs was verified by MALDI TOF MS analysis (Table S1 in the Supporting Information) and ion-pair reverse-phase HPLC, respectively.

The hybridization characteristics of ONs modified with **W–Z** monomers were examined in 13-mer sequence contexts that have previously been used to study base-discriminating fluorescent ONs.<sup>13,15,48</sup> Nucleotides flanking the **W–Z** monomers were systematically varied to explore the influence of sequence context on hybridization characteristics (Table 1). The thermostability of duplexes was evaluated by determining their thermal denaturation temperature (*T*<sub>m</sub>) in a medium salt buffer ([Na<sup>+</sup>] = 110 mM, pH 7.0). Changes in *T*<sub>m</sub> values of modified duplexes are discussed relative to *T*<sub>m</sub> values of

Table 1.  $T_m$  Values of Duplexes between Centrally Modified ONs and Complementary or Centrally Mismatched DNA Targets<sup>a</sup>

ON	sequence	B=	$T_m$ ( $\Delta T_m$ ) [°C]			avg. mismatch $\Delta T_m$ seq. [°C]	avg. mismatch $\Delta T_m$ series [°C]
			A	C	G		
1	5'-CGCAA ATA AACGC		48.5	-10.0	-5.0	-9.0	-8.0 ± 2.6
2	5'-CGCAA CTC AACGC		55.5	-13.5	-9.5	-9.0	-10.7 ± 2.5
3	5'-CGCAA GTG AACGC		55.5	-13.0	-9.5	-10.0	-10.8 ± 1.9
4	5'-CGCAA TTT AACGC		48.5	-11.0	-9.0	-11.0	-10.3 ± 1.2
5	5'-CGCAA AWA AACGC		48.0 (-0.5)	+1.0	+1.5	+1.5	+1.3 ± 0.3
6	5'-CGCAA CWC AACGC		53.5 (-2.0)	+0.5	+2.0	+2.5	+1.7 ± 1.0
7	5'-CGCAA GWG AACGC		51.5 (-4.0)	+1.0	-4.5	0.0	-1.2 ± 2.9
8	5'-CGCAA TWT AACGC		47.0 (-1.5)	+2.5	-0.5	+2.0	+1.3 ± 1.6
9	5'-CGCAA AXA AACGC		46.5 (-2.0)	+1.0	+0.5	+1.0	+0.8 ± 0.3
10	5'-CGCAA CXC AACGC		52.0 (-3.5)	-1.5	0.0	-0.5	-0.7 ± 0.8
11	5'-CGCAA GXG AACGC		52.5 (-3.0)	+0.5	-7.0	-0.5	-2.3 ± 4.1
12	5'-CGCAA TXT AACGC		44.5 (-4.0)	+1.0	-1.0	0.0	0.0 ± 1.0
13	5'-CGCAA AYA AACGC		49.5 (+1.0)	+1.5	0.0	+1.0	+0.8 ± 0.8
14	5'-CGCAA CYC AACGC		50.5 (-5.0)	-5.0	-1.0	-2.5	-2.8 ± 2.0
15	5'-CGCAA GYG AACGC		53.0 (-2.5)	+1.5	-3.5	+0.5	-0.5 ± 2.6
16	5'-CGCAA TYT AACGC		44.5 (-4.0)	-2.0	-2.0	-1.5	-1.8 ± 0.3
17	5'-CGCAA AZA AACGC		47.0 (-1.5)	-5.5	-2.5	-4.0	-4.0 ± 1.5
18	5'-CGCAA CZC AACGC		51.5 (-4.0)	-6.5	-1.0	-4.0	-3.8 ± 2.8
19	5'-CGCAA GZG AACGC		52.0 (-3.5)	-2.0	-6.0	-4.0	-4.0 ± 2.0
20	5'-CGCAA TZT AACGC		45.5 (-3.0)	-4.5	-5.0	-4.0	-4.5 ± 0.5

<sup>a</sup> $T_m$  values determined as maximum of the first derivative of denaturation curves ( $A_{260}$  vs  $T$ ) recorded in thermal denaturation buffer ( $[\text{Na}^+] = 110$  mM,  $[\text{Cl}^-] = 100$  mM, pH 7.0 ( $\text{NaH}_2\text{PO}_4/\text{Na}_2\text{HPO}_4$ )) using 1.0  $\mu\text{M}$  of each strand.  $T_m$  values are averages of at least two measurements within 1.0 °C.  $\Delta T_m$  = change in  $T_m$  relative to unmodified reference duplex. Mismatch  $\Delta T_m$  = change in  $T_m$  relative to fully matched duplex (B = A). Avg. mismatch  $\Delta T_m$  seq = average of all three mismatch  $\Delta T_m$  values for a given probe. Avg. mismatch  $\Delta T_m$  series = average of all 12 mismatch  $\Delta T_m$  values of all four studied probe contexts within a monomer series;  $\pm$  denotes standard deviation. DNA targets: 3'-GCGTT TBT TTGCG (for ON1/ON5/ON9/ON13/ON17), 3'-GCGTT GBG TTGCG (for ON2/ON6/ON10/ON14/ON18), 3'-GCGTT CBC TTGCG (for ON3/ON7/ON11/ON15/ON19), and 3'-GCGTT ABA TTGCG (for ON4/ON8/ON12/ON16/ON20). For structures of monomers W–Z, see Figure 1.

unmodified reference duplexes ( $\Delta T_m$ ). The exchange of thymine (reference ONs) with uracil moieties (modified ONs) results in a decrease of 0.5 °C per incorporation<sup>49</sup> by itself but is not considered further herein.

**Thermal Denaturation Studies.** Thermal denaturation curves of DNA duplexes modified with C2'-pyrene-functionalized triazole-linked 2'-deoxyuridine monomers W–Z display similar sigmoidal monophasic transitions as unmodified reference duplexes (Figure S1). ONs that are centrally modified with a single W–Z monomer generally display moderately decreased thermal affinity toward complementary DNA ( $\Delta T_m$  for ON5–ON20 between -5.0 and +1.0 °C, Table 1). Less pronounced destabilization is observed for (a) ONs modified with monomer W where the pyrene is directly linked to the triazole moiety, and (b) ONs with a central ABA-context (ON5/ON9/ON13/ON17).

Control studies using 9-mer ONs revealed that monomer V, which lacks a pyrene moiety, induces larger decreases in duplex thermostability than pyrene-functionalized monomer Z (difference in  $T_m$  values = 2.5–4.5 °C, Table S2). This indicates that the C2'-triazole moiety is the primary destabilizing structural element of the W–Z monomers.

The Watson–Crick specificity of singly modified ON5–ON20 was studied using DNA targets with mismatched nucleotides opposite of the modification site. Interestingly, ON5–ON12 (monomers W/X) display extremely robust *universal hybridization characteristics*; that is, mismatched

duplexes exhibit minimal changes in  $T_m$  values relative to matched duplexes (mismatch  $\Delta T_m$  values between -1.5 and +2.5 °C, Table 1). ONs with a GBG context that are hybridized to dG-mismatched targets are the exception hereto (see mismatch  $\Delta T_m$  values for ON7 and ON11, Table 1). Thus, the average mismatch  $\Delta T_m$  values across the four studied sequence contexts are +0.8 and -0.5 °C for ONs modified with monomer W and X, respectively. In contrast, unmodified reference strands ON1–ON4 display the expected mismatch discrimination profile including (a) formation of substantially destabilized mismatched duplexes (average mismatch  $\Delta T_m$  = -10.0 °C, Table 1) and (b) more efficient discrimination of pyrimidine–pyrimidine mismatches than of pyrimidine–purine mismatches. ONs modified with monomer Y, where the pyrene and triazole moieties are separated by a flexible two-carbon linker (ON13–ON16), also display universal hybridization characteristics albeit with slightly greater sequence- and mismatch-dependent variation than observed for ON5–ON12 (average mismatch  $\Delta T_m$  = -1.1 °C, Table 1). ONs modified with monomer Z, which has the longest linker studied herein, do not display universal hybridization characteristics. However, markedly reduced discrimination of mismatched targets is still observed (compare mismatch  $\Delta T_m$  values for ON17–ON20 and ON1–ON4, Table 1).

We have previously studied ONs modified with C5'-pyrene-functionalized triazole-linked 2'-deoxyuridine monomers in identical sequence contexts and found them to display similar

Table 2.  $T_m$  Values of Duplexes between ON21–ON33 and Complementary or Centrally Mismatched DNA Targets<sup>a</sup>

ON	sequence	B=	DNA: 5'-CGCAA ABA AACGC			
			$T_m$ ( $\Delta T_m$ ) [°C]	mismatch $\Delta T_m$ [°C]		
			T	A	C	G
21	3'-GCGTT TAT TTGCG		48.5	-10.0	-10.0	-5.5
22	3'-GCGTT TAW TTGCG		46.5 (-2.0)	-17.0	-9.0	-12.0
23	3'-GCGTT WAT TTGCG		41.0 (-7.5)	-11.5	-10.0	-5.5
24	3'-GCGTT WAW TTGCG		35.0 (-13.5)	nt	-3.5	nt
25	3'-GCGTT TAX TTGCG		44.0 (-4.5)	-9.0	-7.5	-5.0
26	3'-GCGTT XAT TTGCG		42.0 (-6.5)	-10.5	-11.5	-6.0
27	3'-GCGTT XAX TTGCG		36.5 (-12.0)	-2.5	-4.5	+0.5
28	3'-GCGTT TAY TTGCG		40.0 (-8.5)	-7.0	-7.0	-5.0
29	3'-GCGTT YAT TTGCG		42.5 (-6.0)	-6.0	-2.5	-7.0
30	3'-GCGTT YAY TTGCG		34.5 (-14.0)	-4.5	-3.5	-4.5
31	3'-GCGTT TAZ TTGCG		42.5 (-6.0)	-7.0	-8.5	-7.5
32	3'-GCGTT ZAT TTGCG		44.0 (-4.5)	-11.5	-12.0	-9.0
33	3'-GCGTT ZAZ TTGCG		39.5 (-9.0)	-2.5	-0.5	-3.5

<sup>a</sup>Conditions and definitions as described in footnote of Table 1; nt = no transition.

mismatch  $\Delta T_m$  values as ONs modified with monomer W/X/Y; however, significantly greater duplex destabilization was observed (average  $\Delta T_m \sim -7.5$  °C).<sup>13</sup> In contrast, ONs modified with the related 2'-O-(pyren-1-yl)methyluridine or 2'-N-(pyren-1-ylmethyl)-2'-N-methylaminouridine monomers display very high thermal affinity toward complementary DNA and do not display universal hybridization characteristics.<sup>21</sup> These observations suggest that pyrene-functionalized triazole moieties are structural units that promote universal hybridization characteristics, and that their specific attachment point on the nucleotide influences duplex thermostability.

Next, ON22–ON33 were prepared to study how incorporation of W–Z monomers as next-nearest neighbors influences duplex thermostability and if the presence of W–Z monomers influences the discriminatory ability of the neighboring nucleoside for its Watson–Crick complement (Table 2).<sup>50</sup> Singly modified ONs with TBA and ABT contexts display lower thermal affinity toward complementary DNA than ONs with symmetric ABA or TBT contexts (e.g., compare  $\Delta T_m$  values for ON5, ON8, ON22, and ON23, Table 2). This underscores the general point that new nucleotide monomers must be studied in many different sequence contexts before a full understanding of hybridization effects is reached. Incorporation of a second X–Z monomer results in approximately additive decreases in duplex thermostability, while greater-than-additive decreases are observed with monomer W (e.g., compare  $\Delta T_m$  values for ON22/ON23/ON24, Table 2).

The presence of a single W–Z monomer has, with few exceptions (ON22/ON29), only a minor effect on the discriminatory ability of neighboring base pairs (e.g., compare mismatch  $\Delta T_m$  values for ON31/ON32 relative to ON21, Table 2). This reduces the risk of nonspecific target binding and suggests that the pyrene-functionalized triazole units of W–Z monomers do not interact strongly with neighboring base pairs. Doubly modified ONs display poor discrimination of DNA targets with mismatched nucleotides positioned between the modification sites (e.g., compare mismatch  $\Delta T_m$

values for ON33 relative to ON21, Table 2), although these trends cannot be categorized as universal hybridization. We speculate that the poor mismatch specificity is caused by the dynamic local duplex structure that arises as a consequence of the low duplex thermostability.

In summary, the data demonstrate that ONs modified with C2'-pyrene-functionalized triazole-linked 2'-deoxyuridine monomers display universal hybridization characteristics with DNA targets that have mismatched nucleotides opposite of the modification site (compare mismatch  $\Delta T_m$  values in Tables 1 and 2 but only have limited influence on the Watson–Crick specificity of neighboring base pairs).

As a first step toward rationalizing whether intercalation of the pyrene/triazole moieties of monomers W–Z governs the observed universal hybridization characteristics, we hybridized ON4/ON8/ON12/ON16/ON20 (TBT context) to DNA targets containing a THF-type abasic site monomer  $\Phi$ <sup>51</sup> opposite of monomers W–Z (for structure of monomer  $\Phi$ , see Figure 1). As expected, the duplex between reference strand ON4 and the abasic target strand is greatly destabilized relative to the matched duplex due to perturbation of the base stack (abasic  $\Delta T_m = -20.0$  °C, Table 3). In contrast, ONs modified with monomers W–Z result in the formation of remarkably thermostable duplexes with abasic target strands (abasic  $\Delta T_m$  between -3.5 and +4.5 °C, Table 3). The observed trend in abasic  $\Delta T_m$  values (W > X > Y > Z) demonstrates that monomers with progressively longer linkers between the pyrene and triazole moieties result in progressively less pronounced stabilization of abasic sites.

Stabilization of abasic sites has previously been observed for monomers with extended aromatic units which occupy the void formed by an abasic site and re-establish  $\pi$ – $\pi$  stacking at the lesion site.<sup>18,35,52–54</sup> Full restoration of duplex thermostability, however, is rarely observed. These observations indicate that the pyrene and/or triazole moieties of monomers W–Z are intercalating into the duplex core and thereby disrupt interactions between mismatched base pairs, leading to a lack



**Table 3.**  $T_m$  Values of Duplexes between Centrally Modified ONs (TBT Context) and Complementary DNA or Targets Containing a Central Abasic Site<sup>a</sup>

ON	sequence	3'-GCGTT ATA TTGCG	
		$T_m$ [°C]	abasic $\Delta T_m$ [°C]
4	5'-CGCAA TTT AACGC	48.5	-20.0
8	5'-CGCAA TWT AACGC	47.0	+4.5
12	5'-CGCAA TXT AACGC	44.5	+2.0
16	5'-CGCAA TYT AACGC	44.5	+0.5
20	5'-CGCAA TZT AACGC	45.5	-3.5

<sup>a</sup>Conditions as described in footnote of Table 1. Abasic  $\Delta T_m$  = change in  $T_m$  relative to fully matched duplex;  $\Phi$  = abasic monomer (for structure, see Figure 1).

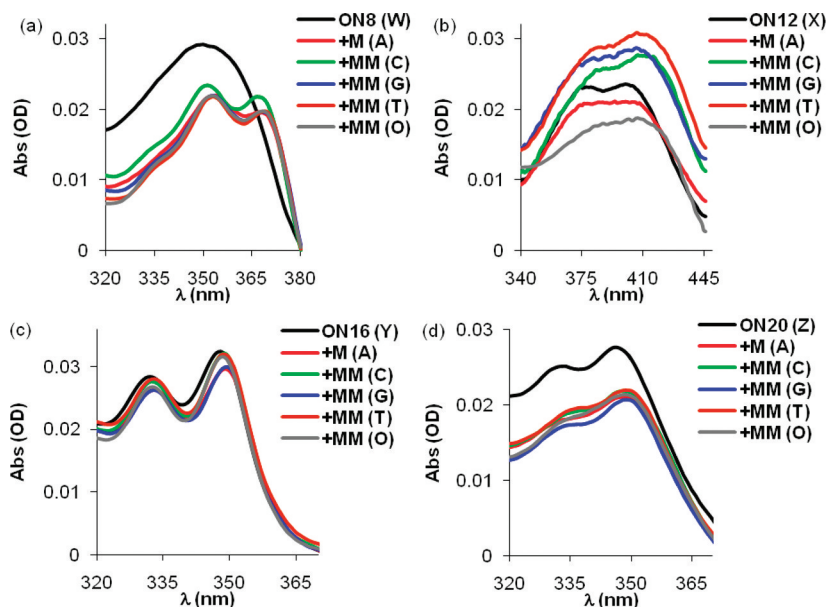


**Figure 2.** Representative absorption spectra of single-stranded ON8/ON12/ON16/ON20 (a–d) and their duplexes with matched (M) and centrally mismatched (MM) DNA targets: 3'-GCGTT ABA TTGCG. Nucleotide opposite of modification is mentioned in parentheses. Spectra were recorded in thermal denaturation buffer at  $T = 20$  °C using 1.0  $\mu\text{M}$  concentration of each strand. Note that different  $x$ -axes are used. "O" denotes THF-type abasic site monomer  $\Phi$  (Figure 1).

of thermal preference for a particular nucleotide opposite of the modification site.

**Optical Spectroscopy Studies.** UV–vis absorption spectra of ONs modified with monomers W–Z were recorded in the absence or presence of complementary or centrally mismatched DNA targets in order to gain additional insights into the mechanism that governs the observed universal hybridization characteristics (Figure 2); hybridization-induced intercalation of pyrene moieties is known to induce subtle bathochromic shifts.<sup>55</sup>

Single-stranded ON5–ON8 (monomer W) display a single unstructured maximum in the pyrene region ( $\lambda_{\text{max}} \sim 351$  nm, Figure 2), while duplexes with complementary, mismatched, or abasic DNA targets display two resolved maxima at  $\sim 351$  and  $\sim 365$  nm. The lack of defined peaks for the single-stranded probes (SSPs) precludes analysis of bathochromic shifts. Single-stranded ON9–ON12 (monomer X) display two broad and virtually equally intense peaks, which renders exact determination of absorption maxima difficult ( $\lambda_{\text{max}} \sim 385$  and  $\sim 415$  nm, Figure 2). Hybridization with complementary DNA results in subtle bathochromic shifts, while more pronounced shifts are observed upon hybridization with mismatched or abasic DNA. The pyrene maxima of ON5–ON12 are red-shifted relative to those of unconjugated pyrene chromophores,<sup>13,19,21</sup> which

suggests electronic coupling between the pyrene and triazole moieties. Single-stranded ON13–ON16 (monomer Y) and ON17–ON20 (monomer Z), on the other hand, have structured absorption spectra with two maxima in the "normal" region (i.e.,  $\lambda_{\text{max}} \sim 333/348$  and  $\sim 332/346$  nm, respectively, Figure 2). Hybridization of ON13–ON20 with complementary, mismatched, or abasic DNA target strands results in subtle bathochromic shifts ( $\Delta\lambda_{\text{max}}$  between +1 and +3 nm, Figure 2 and Table S3). Thus, the absorption data are consistent with the hypothesis that the pyrene moieties of monomers W–Z intercalate into the duplex core upon hybridization with DNA targets.

Next, steady-state fluorescence emission spectra and fluorescence emission quantum yields were determined for ON5–ON20 in the absence or presence of complementary or centrally mismatched DNA targets (Figure 3 and Table 4).

**Monomer W.** Single-stranded ON5–ON8 display two structured emission peaks at  $\lambda_{\text{em}} \sim 390$  and 405 nm (Figure 3). The single-stranded probe with a central AWA context (ON5) has higher fluorescence quantum yield than SSPs in other contexts ( $\Phi_{\text{F}} = 0.27$  vs 0.07/0.05/0.05, Table 4; see also Figure S2). This is in agreement with previous observations that adenine is the weakest quencher of pyrene fluorescence (quenching trend: G > C > T > A).<sup>15,56,57</sup> The

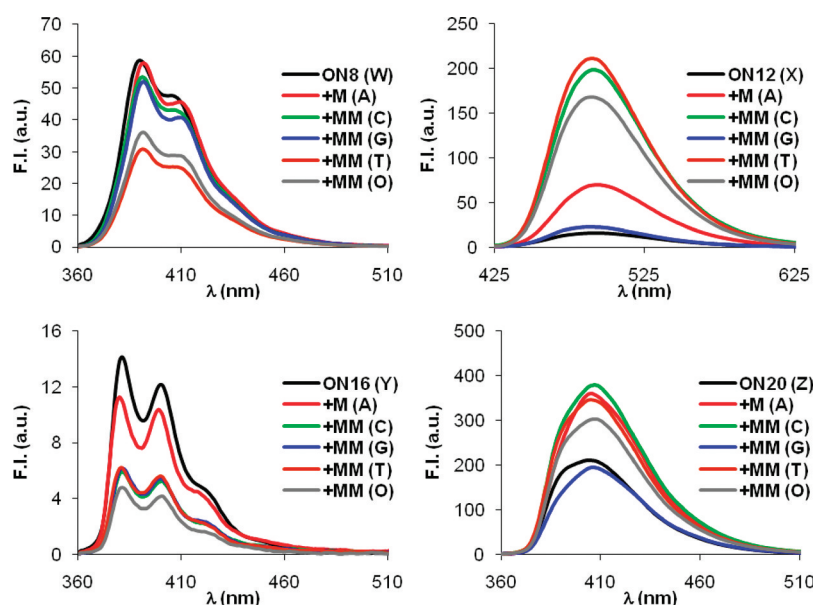


**Figure 3.** Steady-state fluorescence emission spectra of single-stranded ON8/ON12/ON16/ON20 (TTT context) and duplexes with matched (M) or centrally mismatched (MM) DNA. Recorded in thermal denaturation buffer at  $T = 20\text{ }^{\circ}\text{C}$  using  $1.0\text{ }\mu\text{M}$  of each strand and  $\lambda_{\text{ex}} = 350\text{ nm}$  (monomers W, Y, and Z) or  $\lambda_{\text{ex}} = 400\text{ nm}$  (monomer X). DNA targets 3'-GCGTT ABA TTGCG. Nucleotide opposite of modification is mentioned in parentheses. Note that different axes are used. "O" denotes THF-type abasic site monomer  $\Phi$  (Figure 1).

**Table 4. Relative Fluorescence Emission Quantum Yield ( $\Phi_{\text{F}}$ ) of ON5–ON20 in the Absence (SSP) or Presence of Matched (M) or Centrally Mismatched (MM) DNA Targets<sup>a</sup>**

ON	sequence	$\Phi_{\text{F}}$				
		SSP	+M (A)	+MM (C)	+MM (G)	+MM (T)
5	5'-CGCAA AWA AACGC	0.27	0.08	0.09	0.06	0.08
6	5'-CGCAA CWC AACGC	0.07	0.02	0.02	0.02	0.01
7	5'-CGCAA GWG AACGC	0.05	0.03	0.01	0.02	0.01
8	5'-CGCAA TWT AACGC	0.05	0.07	0.06	0.06	0.04
9	5'-CGCAA AXA AACGC	0.02	0.25	0.33	0.10	0.25
10	5'-CGCAA CXC AACGC	0.02	<0.01	<0.01	<0.01	<0.01
11	5'-CGCAA GXG AACGC	<0.01	<0.01	<0.01	<0.01	<0.01
12	5'-CGCAA TXT AACGC	0.04	0.16	0.35	0.04	0.32
13	5'-CGCAA AYA AACGC	0.09	0.02	0.02	0.02	0.03
14	5'-CGCAA CYC AACGC	0.01	0.02	<0.01	<0.01	<0.01
15	5'-CGCAA GYG AACGC	0.03	0.01	0.01	0.01	<0.01
16	5'-CGCAA TYT AACGC	0.01	<0.01	<0.01	<0.01	<0.01
17	5'-CGCAA AZA AACGC	0.58	0.52	0.78	0.29	0.79
18	5'-CGCAA CZC AACGC	0.24	0.15	0.17	0.15	0.19
19	5'-CGCAA GZG AACGC	0.05	0.04	0.02	0.02	0.03
20	5'-CGCAA TZT AACGC	0.27	0.57	0.58	0.31	0.52

<sup>a</sup>Relative to quantum yield of anthracene in ethanol (0.27). Recorded in thermal denaturation buffer at  $T = 20\text{ }^{\circ}\text{C}$  using  $1.0\text{ }\mu\text{M}$  concentration of each strand and  $\lambda_{\text{ex}} = 350\text{ nm}$  and  $\lambda_{\text{em}} = 360\text{--}510\text{ nm}$  (monomers W, Y, and Z) or  $\lambda_{\text{ex}} = 400\text{ nm}$  and  $\lambda_{\text{em}} = 425\text{--}625\text{ nm}$  (monomer X). For DNA targets, see footnote of Table 1. Nucleotide opposite of modification is mentioned in parentheses.

spectra of the corresponding duplexes with complementary DNA have a similar shape and sequence dependency, underlining that the pyrene moiety is in close contact with the neighboring nucleobases (Figure 3 and Table 4). The extensive decreases in fluorescence quantum yield (Table 4 and Figure S3) upon hybridization with matched or mismatched DNA targets further corroborates this hypothesis. ON8 (TWT context) exhibits considerably smaller changes, presumably since the fluorophore interacts with the

neighboring and only weakly quenching adenine moieties upon target binding (Figure 3 and Figure S3).

**Monomer X.** Fluorescence emission spectra of single-stranded ON9–ON12 and the corresponding duplexes with complementary or mismatched DNA targets display broad and unstructured emission peaks with maxima at  $\lambda_{\text{em}} \sim 490\text{ nm}$  (Figure 3). SSPs are strongly quenched with ON11 (GXG context) displaying the lowest intensity ( $\Phi_{\text{F}} < 0.04$ , Table 4 and Figure S2). Quantum yields are markedly increased upon

hybridization of **ON9** or **ON12** with complementary/mismatched DNA targets (Table 4 and Figure S3). In contrast, **ON10** or **ON11** display hybridization-induced decreases in fluorescence intensity (Table 4 and Figure S3). One interpretation of these observations is that the conjugated pyrene moiety of monomer **X** intercalates into the base stack where it is quenched by neighboring cytosine and guanine moieties (**ON10/ON11**) but not quenched by adenine and thymine moieties (**ON9/ON12**). An alternative interpretation is that the pyrene moiety of monomer **X** only intercalates with **ON10/ON11**. However, the similar influence on duplex thermostability upon incorporation of monomer **X** irrespective of sequence context (compare  $\Delta T_m$  values for **ON9–ON12**, Table 1) and the hybridization-induced bathochromic shifts of pyrene absorption peaks (Figure 2) are in stronger support of the first interpretation.

**Monomer Y.** The fluorescence emission spectra of **ON13–ON16** and the corresponding duplexes with matched or mismatched DNA targets display two well-resolved pyrene peaks at  $\lambda_{em} \sim 380$  and  $400$  nm, with an additional shoulder at  $\lambda_{em} \sim 420$  nm (Figure 3). Very low quantum yields are observed ( $\Phi_F < 0.03$ , Table 4), except for the single-stranded **ON13** (AYA context). Hybridization of **ON13–ON16** with complementary or mismatched DNA targets generally results in decreased fluorescence intensity (Figure S3), which is consistent with an intercalating binding mode for the pyrene moiety.

**Monomer Z.** The fluorescence emission spectra of single-stranded **ON17–ON20** and the corresponding duplexes with matched or mismatched DNA targets display an unstructured peak at  $\lambda_{em} \sim 410$  nm with a weaker shoulder at  $\lambda_{em} \sim 390$  nm (Figure 3). The quantum yields of SSPs range from moderate to high and closely align with the previously discussed quenching trends of nucleobases ( $\Phi_F = 0.05–0.58$ , Table 4 and Figure S2). Hybridization with matched or mismatched DNA targets generally results in decreases (CZC/GZG contexts) or minor increases (AZA/TZT contexts) in quantum yields and intensity (Table 4 and Figure S3), which resembles the trends with **ON9–ON12**.

Perhaps the most important observation toward rationalizing the universal hybridization properties of **ON5–ON20** is that very similar quantum yields are observed for the four duplexes between a particular probe and matched/mismatched DNA targets (e.g., compare  $\Phi_F = 0.08/0.09/0.06/0.08$  for **ON5** vs matched/mismatched DNA targets, Table 4). **ON9**, **ON12**,

**ON17**, and **ON20** are exceptions hereto as lower quantum yields are observed upon hybridization with dG-mismatched targets than with other DNA targets; however, this most likely reflects the fact that guanine is a strong fluorophore quencher.<sup>56</sup> Collectively, these observations indicate (a) that the fluorophore is in a similar electronic environment within the duplex core regardless of the nucleotide opposite of the monomer and, therefore, (b) that the opposing nucleotide is not strongly involved in base pairing and possibly even pushed into an extrahelical position (Figure 4). Along the lines, it is

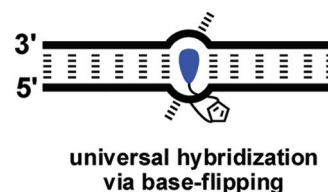


**Figure 4.** Illustration of putative mechanism resulting in universal hybridization.

interesting to note that placement of pyrene-functionalized C-glycosides in DNA duplexes opposite of abasic sites, which are generated via enzyme-mediated extrahelical flipping of the opposing nucleotide, is known to be stabilizing.<sup>58,59</sup>

**Universal Hybridization—RNA Targets.** A representative subset of modified ONs (TBT/CBT contexts) was studied with respect to thermal denaturation, absorption, and fluorescence properties with complementary/mismatched RNA targets. The following observations were made: (a) incorporation of monomer **W** or **X** into ONs results in similar decreases in thermal affinity toward complementary RNA as toward DNA, while ONs modified with monomers **Y** or **Z** have lower affinity toward RNA (Table 5 and Figure S4); (b) ONs modified with monomers **W** or **X** display robust universal hybridization characteristics (compare mismatch  $\Delta T_m$  values for **ON6/ON8/ON12** and **ON2/ON4**, Table 5), while ONs modified with monomers **Y** or **Z** do not; (c) pyrene absorption spectra of duplexes between modified ONs and complementary or centrally mismatched RNA targets are very similar to those of the corresponding DNA duplexes (compare Figure S5 and Figure 2); hybridization-induced bathochromic shifts with **ON14/ON16/ON18/ON20** (monomer **Y/Z**) are more subtle

**Table 5.**  $T_m$  Values of Duplexes between Centrally Modified ONs and Complementary or Centrally Mismatched RNA Targets<sup>a</sup>

ON	sequence	B=	$T_m$ ( $\Delta T_m$ ) [°C]		mismatch $\Delta T_m$ [°C]		
			A	C	G	U	
2	5'-CGCAA CTC AACGC		51.5	-15.5	-3.0	-13.5	
4	5'-CGCAA TTT AACGC		40.5	-19.0	-3.5	-17.0	
6	5'-CGCAA CWC AACGC		47.0 (-4.5)	+1.0	+0.0	+0.5	
8	5'-CGCAA TWT AACGC		42.0 (+1.5)	+3.0	+0.5	+1.5	
12	5'-CGCAA TXT AACGC		38.0 (-2.5)	+1.0	+0.0	+1.0	
14	5'-CGCAA CYC AACGC		43.5 (-8.0)	-2.0	-5.0	-4.0	
16	5'-CGCAA TYT AACGC		36.0 (-4.5)	+1.5	-1.0	-1.0	
18	5'-CGCAA CZC AACGC		44.5 (-7.0)	-3.0	-8.0	-7.0	
20	5'-CGCAA TZT AACGC		36.5 (-4.0)	-12.0	-7.5	-13.0	

<sup>a</sup>Conditions and definitions as described in footnote of Table 1. RNA targets: 3'-GCGUU GBG UUGCG (for **ON2/ON6/ON14/ON18**) and 3'-GCGUU ABA UUGCG (for **ON4/ON8/ON12/ON16/ON20**).



with RNA targets than with the corresponding DNA targets (compare Table S4 and Table S3); and (d) hybridization of modified ONs to RNA targets results in very similar changes in fluorescence intensity as with DNA targets (compare Figure S6 and Figure S3).

Thus, the results indicate that the universal RNA hybridization characteristics of ONs modified with monomer W/X (ON6/ON8/ON12/ON20) are governed by a similar mechanism as universal DNA hybridization (Figure 4).

## CONCLUSION

Oligodeoxyribonucleotides modified with C2'-pyrene-functionalized triazole-linked 2'-deoxyuridine monomers display highly robust universal hybridization characteristics without markedly compromising duplex thermostability (Tables 1 and 5), which sets them apart from probes based on conventional universal bases such as 3-nitropyrrole or 5-nitroindole. Thermal denaturation and optical spectroscopy data suggest the universal hybridization characteristics to be a consequence of pyrene intercalation whereby the nucleotide opposite of the monomer is pushed out (Figure 4). Given the straightforward access to this monomer class via the Cu<sup>I</sup>-catalyzed [3 + 2] azide-alkyne cycloaddition reaction (Scheme 2), the stage is set for detailed structure-property studies for refinement of hybridization characteristics (e.g., attachment of other aromatic moieties) and biotechnological exploration of these universal hybridization probes as degenerate PCR primers and microarray probes.

## EXPERIMENTAL SECTION

**General.** Reagents and solvents were obtained from commercial vendors, of analytical grade, and used without further purification. Petroleum ether of the distillation range 60–80 °C was used. Solvents were dried over activated molecular sieves: CH<sub>2</sub>Cl<sub>2</sub> and *N,N'*-diisopropylethylamine (4 Å). Water content of anhydrous solvents was verified using Karl Fischer apparatus. Reactions were conducted under argon whenever anhydrous solvents were used. Reactions were monitored by TLC using silica gel coated plates with a fluorescence indicator (SiO<sub>2</sub>-60, F-254) and were visualized (a) under UV light and/or (b) by dipping in 5% concd H<sub>2</sub>SO<sub>4</sub> in absolute ethanol (v/v) followed by heating. Silica gel column chromatography was performed with silica gel 60 (particle size 0.040–0.063 mm) using moderate pressure (pressure ball). Evaporation of solvents was carried out under reduced pressure at temperatures below 45 °C. After column chromatography, appropriate fractions were pooled, evaporated, and dried at high vacuum for at least 12 h to give the obtained products in high purity (>95%) as ascertained by 1D NMR techniques. Chemical shifts of <sup>1</sup>H NMR (500 MHz), <sup>13</sup>C NMR (125.6 MHz), <sup>31</sup>P NMR (121.5 MHz), and/or <sup>19</sup>F NMR (282.2 MHz) signals are reported relative to deuterated solvent or other internal standards (80% phosphoric acid for <sup>31</sup>P NMR). Exchangeable (ex) protons were detected by disappearance of <sup>1</sup>H NMR signals upon D<sub>2</sub>O addition. Assignments of NMR spectra are based on 2D spectra (HSQC, COSY) and DEPT spectra. Quarternary carbons are not assigned in <sup>13</sup>C NMR but verified from DEPT spectra (absence of signals). MALDI-HRMS spectra of compounds were recorded on a Q-TOF mass spectrometer using 2,5-dihydroxybenzoic acid (DHB) as a matrix and polyethylene glycol (PEG 600) as an internal calibration standard.

**1-(Pyren-1-yl)-prop-2-yn-1-ol (Ax').** Trimethylsilylacetylene (1.0 mL, 7.00 mmol) was added to MeMgBr in THF (1M, 4.0 mL, 4.00 mmol) under an argon atmosphere and stirred at rt for 1 h. At this point, pyrene-1-carboxaldehyde (0.70 g, 3.00 mmol) was added and the reaction mixture was stirred at rt for another 2 h. Saturated aqueous NH<sub>4</sub>Cl (~1 mL) was added, and the mixture was extracted with EtOAc (2 × 20 mL). The combined organic phase was dried over Na<sub>2</sub>SO<sub>4</sub> and evaporated to dryness. The resulting crude [assumed to be 1-(pyren-1-yl)-3-trimethylsilyl-prop-2-yn-1-ol] was dissolved in

CH<sub>2</sub>Cl<sub>2</sub> and MeOH (10 mL, 1:1, v/v) and stirred with K<sub>2</sub>CO<sub>3</sub> (0.50 g, 3.62 mmol) at rt for 2 h. The reaction mixture was then diluted with CH<sub>2</sub>Cl<sub>2</sub> (10 mL) and successively washed with brine (20 mL) and water (20 mL). The organic phase was dried over Na<sub>2</sub>SO<sub>4</sub> and evaporated to dryness. The resulting crude was purified by silica gel column chromatography (0–50% EtOAc in petroleum ether, v/v) to afford Ax' (0.47 g, 58%) as a white solid material: *R*<sub>f</sub> = 0.3 (25% EtOAc in petroleum ether, v/v); ESI-HRMS *m/z* 279.0783 ([M + Na]<sup>+</sup>, C<sub>19</sub>H<sub>12</sub>O·Na<sup>+</sup>, calcd 279.0780); <sup>1</sup>H NMR (DMSO-*d*<sub>6</sub>) δ 8.59 (d, 1H, *J* = 10.0 Hz, Py), 8.35–8.29 (m, 4H, Py), 8.26 (d, 1H, *J* = 10.0 Hz, Py), 8.20–8.16 (m, 2H, Py), 8.09 (t, 1H, *J* = 7.5 Hz, Py), 6.41–6.39 (d, 1H, ex, *J* = 5.0 Hz, OH), 6.34–6.31 (dd, 1H, *J* = 5.0 Hz, 2.5 Hz, HC(OH)), 3.60 (d, 1H, *J* = 2.5 Hz, HC≡C); <sup>13</sup>C NMR (DMSO-*d*<sub>6</sub>) δ 135.0, 130.7, 130.5, 130.1, 127.34, 127.31 (Py), 127.28 (Py), 127.25 (Py), 126.2 (Py), 125.3 (Py), 125.2 (Py), 124.65 (Py), 124.59 (Py), 124.1, 123.8, 123.7 (Py), 85.5, 76.6 (HC≡C), 60.8 (HC(OH)).

**1-(Pyren-1-yl)-prop-2-yn-1-one (Ax).** The Jones reagent (2.67 M CrO<sub>3</sub> in 3 M H<sub>2</sub>SO<sub>4</sub>, 1.0 mL, 2.67 mmol) was added to a solution of alcohol Ax' (180 mg, 0.67 mmol) in acetone (10 mL), and the reaction mixture was stirred under an ambient atmosphere at rt for 2 h, whereupon it was diluted with EtOAc (20 mL), neutralized by dropwise addition of 6 M NaOH (1.0 mL) under stirring, and sequentially washed with water (30 mL) and saturated aqueous NaHCO<sub>3</sub> (30 mL). The organic phase was dried over Na<sub>2</sub>SO<sub>4</sub>, evaporated to dryness, and the resulting crude purified by silica gel column chromatography (0–20% EtOAc in petroleum ether, v/v) to furnish Ax (130 mg, 75%) as a brightly yellow solid material: *R*<sub>f</sub> = 0.6 (50% EtOAc in petroleum ether, v/v); ESI-HRMS *m/z* 277.0626 ([M + Na]<sup>+</sup>, C<sub>19</sub>H<sub>10</sub>O·Na<sup>+</sup>, calcd 277.0624); <sup>1</sup>H NMR (CDCl<sub>3</sub>) δ 9.48 (d, 1H, *J* = 10.0 Hz), 8.94 (d, 1H, *J* = 8.0 Hz), 8.28–8.23 (m, 3H), 8.19–8.14 (m, 2H), 8.07–8.02 (m, 2H), 3.53 (s, 1H); <sup>13</sup>C NMR (CDCl<sub>3</sub>) δ 179.3, 135.8, 132.2 (Py), 131.31, 131.25 (Py), 131.14, 131.05 (Py), 130.6, 128.4, 127.35 (Py), 127.29 (Py), 127.1 (Py), 126.8 (Py), 124.97 (Py), 124.96, 124.95, 124.2 (Py), 124.1, 82.6, 80.1 (HC≡C). We observe distinctly different <sup>1</sup>H NMR signals in the 8.50–8.00 ppm region compared to previous reports on this compound.<sup>60</sup>

**4-(Pyren-1-yl)-but-1-yne (Ay).** An oven-dried flask was charged with pyrene-1-carboxaldehyde (230 mg, 1.00 mmol) and activated zinc (100 mg, 1.50 mmol) and placed under an argon atmosphere. Anhydrous THF (5 mL) and propargyl bromide (0.20 mL, 1.79 mmol) were added, and the reaction mixture was stirred at 45 °C for 4 h. Saturated aqueous NH<sub>4</sub>Cl (1 mL) was added, and the mixture was extracted with EtOAc (2 × 20 mL). The organic phase was washed with brine (20 mL) and evaporated to dryness. The resulting crude was purified by silica gel column chromatography (0–30% EtOAc in petroleum ether, v/v) to afford a crude white solid material (145 mg), which <sup>1</sup>H NMR suggested to be a ~9:1 mixture of the desired 1-(pyren-1-yl)-but-3-yn-1-ol and the corresponding allene. Et<sub>3</sub>SiH (0.20 mL, 1.25 mmol) and boron trifluoride etherate (0.20 mL, 1.62) were added to a solution of the crude mixture in CH<sub>2</sub>Cl<sub>2</sub> (5 mL), which then was stirred at rt for 1 h. The reaction mixture was diluted with CH<sub>2</sub>Cl<sub>2</sub> (20 mL) and saturated aqueous NaHCO<sub>3</sub> (2 mL) and successively washed with brine (20 mL) and water (20 mL). The organic phase was dried over Na<sub>2</sub>SO<sub>4</sub>, evaporated to dryness under reduced pressure, and the resulting crude purified by silica gel column chromatography (0–3% EtOAc in petroleum ether, v/v) to afford Ay (80 mg, 31%) as a white solid material: *R*<sub>f</sub> = 0.5 (5% EtOAc in petroleum ether, v/v); ESI-HRMS *m/z* 277.0973 ([M + Na]<sup>+</sup>, C<sub>20</sub>H<sub>14</sub>·Na<sup>+</sup>, calcd 279.0988); <sup>1</sup>H NMR (CDCl<sub>3</sub>) δ 8.27–8.25 (d, 1H, *J* = 9.5 Hz, Py), 8.17–8.14 (m, 2H, Py), 8.12–8.10 (m, 2H, Py), 8.01 (ap s, 2H), 8.00–7.96 (t, 1H, *J* = 8.0 Hz, Py), 7.92–7.90 (d, 1H, *J* = 7.5 Hz, Py), 3.59 (t, 2H, *J* = 7.7 Hz, CH<sub>2</sub>CH<sub>2</sub>C≡CH), 2.72 (dt, 2H, *J* = 7.7 Hz, 2.5 Hz, CH<sub>2</sub>C≡CH), 2.03 (t, 1H, *J* = 2.5 Hz, HC≡C); <sup>13</sup>C NMR (CDCl<sub>3</sub>) δ 134.7, 131.6, 131.1, 130.5, 128.9, 127.8 (Py), 127.7 (Py), 127.5 (Py), 127.1 (Py), 126.1 (Py), 125.31, 125.27 (Py), 125.2, 125.1 (Py), 125.0 (Py), 123.2 (Py), 84.0, 69.6 (HC≡C), 32.8 (CH<sub>2</sub>CH<sub>2</sub>C≡CH), 21.0 (CH<sub>2</sub>C≡CH).

**General Click Reaction Protocol for Preparation of 2V–2Z (Description for ~6 mmol Scale).** 5'-O-Dimethoxytrityl-2'-azido-2'-deoxyuridine 1<sup>45</sup> and the appropriate alkyne A were added to a



mixture of THF/*t*-BuOH/H<sub>2</sub>O (3:1:1, v/v/v) along with sodium ascorbate and CuSO<sub>4</sub>·5H<sub>2</sub>O (reagent quantities, and solvent volumes are specified below). The reaction mixture was stirred under a nitrogen atmosphere until analytical TLC indicated full conversion (reaction times and temperatures specified below), whereupon it was diluted with EtOAc (10 mL). The organic phase was successively washed with saturated aqueous NaHCO<sub>3</sub> (20 mL) and brine (20 mL), dried over anhydrous Na<sub>2</sub>SO<sub>4</sub>, and evaporated to dryness. The resulting crude was purified by silica column chromatography (eluent specified below) to afford the corresponding nucleoside **2** (yield specified below).

**5'-O-(4,4'-Dimethoxytrityl)-2'-C-[4-(2,2,2-trifluoroacetamidomethyl)-1H-1,2,3-triazol-1-yl]-2'-deoxyuridine (2V).** Nucleoside **1** (0.40 g, 0.70 mmol), 2,2,2-trifluoro-*N*-(prop-2-ynyl)acetamide **Av**<sup>46</sup> (105 mg, 0.70 mmol), sodium ascorbate (70 mg, 0.35 mmol), CuSO<sub>4</sub>·5H<sub>2</sub>O (5 mg, 0.02 mmol), and THF/*t*-BuOH/H<sub>2</sub>O (5 mL) were mixed, reacted (14 h at rt), worked up, and purified (50–100% EtOAc in petroleum ether, v/v) as described above except that the organic phase was successively washed with brine and water. Nucleoside **2V** (0.42 g, 83%) was obtained as a yellow solid material: *R*<sub>f</sub> = 0.3 (80% EtOAc in petroleum ether, v/v); MALDI-HRMS *m/z* 745.2225 ([M + Na]<sup>+</sup>, C<sub>35</sub>H<sub>34</sub>F<sub>3</sub>N<sub>6</sub>O<sub>8</sub>·Na<sup>+</sup>, calcd 745.2204); <sup>1</sup>H NMR (DMSO-*d*<sub>6</sub>) δ 11.40 (d, 1H, ex, *J* = 2.0 Hz, H3), 10.02 (t, 1H, *J* = 6.0 Hz, NHCOCF<sub>3</sub>), 8.01 (s, 1H, Tz), 7.81 (d, 1H, *J* = 8.0 Hz, H6), 7.43–7.22 (m, 9H, DMTr), 6.93–6.88 (m, 4H, DMTr), 6.42 (d, 1H, *J* = 4.5 Hz, H1), 5.79 (d, 1H, ex, *J* = 6.0 Hz, 3'-OH), 5.50 (dd, 1H, *J* = 7.0 Hz, 4.5 Hz, H2'), 5.45 (dd, 1H, *J* = 8.0 Hz, 2.0 Hz, H5), 4.52 (m, 1H, H3'), 4.47 (d, 2H, *J* = 5.5 Hz, CH<sub>2</sub>NHCO), 4.24–4.20 (m, 1H, H4'), 3.75 (s, 6H, CH<sub>3</sub>O), 3.38–3.30 (m, 2H, H5' – partial overlap with H<sub>2</sub>O); <sup>13</sup>C NMR (DMSO-*d*<sub>6</sub>) δ 162.8, 158.09, 158.08, 156.2 (q, <sup>13</sup>J<sub>CF</sub> = 36 Hz, COCF<sub>3</sub>), 150.1, 144.6, 142.4, 140.5 (C6), 135.3, 135.1, 129.7 (DMTr), 127.8 (DMTr), 127.7 (DMTr), 126.7 (DMTr), 124.5 (Tz), 115.8 (q, *J*<sub>CF</sub> = 288 Hz, CF<sub>3</sub>), 113.2 (DMTr), 101.9 (C5), 87.1 (C1'), 85.8, 83.2 (C4'), 68.8 (C3'), 64.5 (C2'), 62.8 (C5'), 55.0 (CH<sub>3</sub>O), 34.5 (CH<sub>2</sub>NHCO); <sup>19</sup>F-NMR (DMSO-*d*<sub>6</sub>) δ -74.2.

**5'-O-(4,4'-Dimethoxytrityl)-2'-C-[4-(pyrene-1-yl)-1H-1,2,3-triazol-1-yl]-2'-deoxyuridine (2W).** Nucleoside **1** (0.28 g, 0.49 mmol), 1-ethynylpyrene **Aw**<sup>47</sup> (130 mg, 0.58 mmol), sodium ascorbate (200 mg, 1.00 mmol), CuSO<sub>4</sub>·5H<sub>2</sub>O (25 mg, 0.10 mmol), and THF/*t*-BuOH/H<sub>2</sub>O (10 mL) were mixed, reacted (7 h at 75 °C), worked up, and purified (40–70% EtOAc in petroleum ether, v/v) as described above to provide nucleoside **2W** (140 mg, 35%) as an off-white solid material: *R*<sub>f</sub> = 0.5 (80% EtOAc in petroleum ether, v/v); MALDI-HRMS *m/z* 820.277 ([M + Na]<sup>+</sup>, C<sub>48</sub>H<sub>39</sub>N<sub>5</sub>O<sub>7</sub>·Na<sup>+</sup>, calcd 820.274); <sup>1</sup>H NMR (DMSO-*d*<sub>6</sub>) δ 11.46 (d, 1H, ex, *J* = 1.5 Hz, NH), 8.87 (d, 1H, *J* = 9.0 Hz, Py), 8.80 (s, 1H, Tz), 8.41–8.33 (m, 4H, Py), 8.27 (d, 1H, *J* = 9.2 Hz, Py), 8.26–8.22 (m, 2H, Py); 8.12 (t, 1H, *J* = 7.5 Hz, Py), 7.91 (d, 1H, *J* = 8.0 Hz, H6), 7.48–7.20 (m, 9H, DMTr), 6.96–6.90 (m, 4H, DMTr), 6.65 (d, 1H, *J* = 5.0 Hz, H1'), 5.95 (d, 1H, ex, *J* = 6.0 Hz, 3'-OH), 5.69 (dd, 1H, *J* = 7.0 Hz, 5.0 Hz, H2'), 5.54 (dd, 1H, *J* = 8.0 Hz, 1.5 Hz, H5), 4.69–4.64 (m, 1H, H3'), 4.40–4.36 (m, 1H, H4'), 3.76 (s, 6H, CH<sub>3</sub>O), 3.46–3.36 (m, 2H, H5'); <sup>13</sup>C NMR (DMSO-*d*<sub>6</sub>) δ 162.9, 158.2, 150.3, 145.7, 144.7, 140.8 (C6), 135.4, 135.2, 130.9, 130.6, 130.3, 129.78 (DMTr), 129.76 (DMTr), 128.0 (Py), 127.9 (DMTr), 127.73 (DMTr), 127.67 (Py), 127.5, 127.3 (Py), 127.0 (Py), 126.8 (DMTr), 126.4 (Py), 125.7 (Tz), 125.5 (Py), 125.16, 125.15 (Py), 125.09 (Py), 124.8 (Py), 124.3, 123.9, 113.3 (DMTr), 102.1 (C5), 87.4 (C1'), 85.9, 83.4 (C4'), 69.1 (C3'), 64.9 (C2'), 63.1 (C5'), 55.0 (CH<sub>3</sub>O).

**5'-O-(4,4'-Dimethoxytrityl)-2'-C-[4-(pyrene-1-ylcarbonyl)-1H-1,2,3-triazol-1-yl]-2'-deoxyuridine (2X).** Nucleoside **1** (0.28 g, 0.49 mmol), 1-(pyren-1-yl)-prop-2-yn-1-one **Ax** (140 mg, 0.55 mmol), sodium ascorbate (200 mg, 1.00 mmol), CuSO<sub>4</sub>·5H<sub>2</sub>O (25 mg, 0.10 mmol), and THF/*t*-BuOH/H<sub>2</sub>O (10 mL) were mixed, reacted (5 h at rt), worked up, and purified (40–90% EtOAc in petroleum ether, v/v) as described above to provide nucleoside **2X** (0.25 g, 60%) as a yellow solid material: *R*<sub>f</sub> = 0.4 (80% EtOAc in petroleum ether, v/v); MALDI-HRMS *m/z* 848.267 ([M + Na]<sup>+</sup>, C<sub>45</sub>H<sub>39</sub>N<sub>5</sub>O<sub>8</sub>·Na<sup>+</sup>, calcd 848.270); <sup>1</sup>H NMR (DMSO-*d*<sub>6</sub>) δ 11.46 (br s, 1H, ex, NH), 8.96 (s, 1H, Tz), 8.51–8.28 (m, 8H, Py), 8.17 (t, 1H, *J* = 7.5 Hz, Py), 7.83 (d, 1H, *J* = 8.0 Hz, H6), 7.44–7.21 (m, 9H, DMTr), 6.93–6.88 (m, 4H, DMTr),

6.55 (d, 1H, *J* = 5.0 Hz, H1'), 5.90 (d, 1H, ex, *J* = 5.0 Hz, 3'-OH), 5.68 (dd, 1H, *J* = 7.0 Hz, 5.0 Hz, H2'), 5.53 (dd, 1H, *J* = 8.0 Hz, 2.0 Hz, H5), 4.64–4.58 (m, 1H, H3'), 4.31–4.26 (m, 1H, H4'), 3.74 (s, 6H, CH<sub>3</sub>O), 3.40–3.30 (m, 2H, H5'); <sup>13</sup>C NMR (DMSO-*d*<sub>6</sub>) δ 188.3, 162.9, 158.1, 150.2, 147.2, 144.6, 140.8 (C6), 135.4, 135.2, 133.0, 131.8, 131.5 (Tz), 130.6, 130.0, 129.74 (DMTr), 129.72 (DMTr), 129.4 (Py), 129.1 (Py), 128.9, 127.9, 127.84 (DMTr), 127.80 (Py), 127.7 (DMTr), 127.2 (Py), 126.8 (Py), 126.7 (DMTr), 126.5 (Py), 126.1 (Py), 124.01 (Py), 123.98 (Py), 123.8, 123.5, 113.2 (DMTr), 102.0 (C5), 87.4 (C1'), 85.8, 83.3 (C4'), 69.0 (C3'), 65.0 (C2'), 63.0 (C5'), 55.0 (CH<sub>3</sub>O).

**5'-O-(4,4'-Dimethoxytrityl)-2'-C-[4-{2-(pyrene-1-yl)ethyl}-1H-1,2,3-triazol-1-yl]-2'-deoxyuridine (2Y).** Nucleoside **1** (0.34 g, 0.60 mmol), 4-(pyren-1-yl)-but-1-yne **Ay** (160 mg, 0.63 mmol), sodium ascorbate (0.25 g, 1.25 mmol), CuSO<sub>4</sub>·5H<sub>2</sub>O (31 mg, 0.12 mmol), and THF/*t*-BuOH/H<sub>2</sub>O (10 mL) were mixed, reacted (2 h at rt), worked up, and purified (50–100% EtOAc in petroleum ether, v/v) as described above to provide nucleoside **2Y** (0.33 g, 67%) as a white solid material: *R*<sub>f</sub> = 0.3 (80% EtOAc in petroleum ether, v/v); MALDI-HRMS *m/z* 848.3046 ([M + Na]<sup>+</sup>, C<sub>50</sub>H<sub>43</sub>N<sub>5</sub>O<sub>7</sub>·Na<sup>+</sup>, calcd 848.3055); <sup>1</sup>H NMR (DMSO-*d*<sub>6</sub>) δ 11.44 (s, 1H, ex, NH), 8.40 (d, 1H, *J* = 9.0 Hz, Py), 8.30–8.19 (m, 4H, Py), 8.13 (ap s, 2H, Py), 8.06 (t, 1H, *J* = 8.0 Hz, Py), 8.01 (s, 1H, Tz), 7.95 (d, 1H, *J* = 8.0 Hz, Py), 7.82 (d, 1H, *J* = 8.0 Hz, H6), 7.44–7.41 (m, 2H, DMTr), 7.36–7.23 (m, 7H, DMTr), 6.94–6.90 (m, 4H, DMTr), 6.44 (d, 1H, *J* = 5.0 Hz, H1'), 5.79 (d, 1H, ex, *J* = 6.0 Hz, 3'-OH), 5.49–5.45 (m, 2H, H5, H2'), 4.54–4.49 (m, 1H, H3'), 4.27–4.22 (m, 1H, H4'), 3.75 (s, 6H, CH<sub>3</sub>O), 3.72–3.66 (m, 2H, CH<sub>2</sub>CH<sub>2</sub>), 3.40–3.30 (m, 2H, H5'), 3.19–3.14 (m, 2H, CH<sub>2</sub>CH<sub>2</sub>); <sup>13</sup>C NMR (DMSO-*d*<sub>6</sub>) δ 162.8, 158.12, 158.11, 150.2, 145.8, 144.6, 140.5 (C6), 135.6, 135.4, 135.1, 130.8, 130.3, 129.7 (DMTr), 129.4, 128.0, 127.8 (DMTr), 127.7 (DMTr), 127.5 (Py), 127.4 (Py), 127.3 (Py), 126.7 (DMTr), 126.5 (Py), 126.1 (Py), 124.93 (Py), 124.88 (Py), 124.8 (Py), 124.2, 124.1, 123.4 (Tz), 123.2 (Py), 113.2 (DMTr), 102.0 (C5), 87.1 (C1'), 85.9, 83.3 (C4'), 68.9 (C3'), 64.3 (C2'), 62.9 (C5'), 55.0 (CH<sub>3</sub>O), 32.6 (CH<sub>2</sub>CH<sub>2</sub>), 27.3 (CH<sub>2</sub>CH<sub>2</sub>).

**5'-O-(4,4'-Dimethoxytrityl)-2'-C-[4-(pyrene-1-yl)-carboxamidomethyl-1H-1,2,3-triazol-1-yl]-2'-deoxyuridine (2Z).** Nucleoside **1** (0.40 g, 0.70 mmol), *N*-(prop-2-ynyl)pyrene-1-carboxamide **Az**<sup>48</sup> (200 mg, 0.71 mmol), sodium ascorbate (50 mg, 0.25 mmol), CuSO<sub>4</sub>·5H<sub>2</sub>O (5 mg, 0.02 mmol), and THF/*t*-BuOH/H<sub>2</sub>O (5 mL) were mixed, reacted (8 h at rt), worked up, and purified (50–100% EtOAc in petroleum ether, v/v) as described above except that the organic phase was successively washed with brine and water. Nucleoside **2Z** (0.49 g, 83%) was obtained as a yellow solid material: *R*<sub>f</sub> = 0.2 (EtOAc); MALDI-HRMS *m/z* 877.2979 ([M + Na]<sup>+</sup>, C<sub>50</sub>H<sub>42</sub>N<sub>6</sub>O<sub>8</sub>·Na<sup>+</sup>, calcd 877.2956); <sup>1</sup>H NMR (DMSO-*d*<sub>6</sub>) δ 11.43 (s, 1H, ex, H3), 9.26 (t, 1H, ex, *J* = 6.0 Hz, NHCO), 8.53–8.52 (d, 1H, *J* = 9.5 Hz, Ar), 8.36–8.34 (m, 3H, Ar), 8.27–8.22 (m, 3H, Ar), 8.17–8.11 (m, 3H, Ar, Tz), 7.85 (d, 1H, *J* = 8.5 Hz, H6), 7.44–7.43 (m, 2H, DMTr), 7.35–7.24 (m, 7H, DMTr), 6.93–6.89 (m, 4H, DMTr), 6.50 (d, 1H, *J* = 4.7 Hz, H1'), 5.87 (d, 1H, ex, *J* = 5.5 Hz, 3'-OH), 5.56 (dd, 1H, *J* = 7.0 Hz, 4.7 Hz, H2'), 5.47 (d, 1H, *J* = 8.0 Hz, H5), 4.71 (d, 2H, *J* = 6.0 Hz, CH<sub>2</sub>NHCO), 4.58–4.54 (m, 1H, H3'), 4.30–4.25 (m, 1H, H4'), 3.75 (s, 6H, CH<sub>3</sub>O), 3.41–3.32 (m, 2H, H5'); <sup>13</sup>C NMR (DMSO-*d*<sub>6</sub>) δ 168.8, 162.9, 158.13, 158.12, 150.2, 144.7, 144.6, 140.5 (C6), 135.4, 135.2, 131.6, 131.5, 130.7, 130.2, 129.8 (DMTr), 128.3 (Ar), 128.1 (Ar), 127.9 (DMTr), 127.8, 127.7 (DMTr), 127.1 (Ar), 126.8 (DMTr), 126.5 (Ar), 125.7 (Ar), 125.5 (Ar), 125.2 (Ar), 124.7 (Ar), 124.3 (Ar), 124.2 (Tz), 123.7, 123.6, 113.2 (DMTr), 102.0 (C5), 87.1 (C1'), 85.9, 83.3 (C4'), 69.0 (C3'), 64.5 (C2'), 62.9 (C5'), 55.0 (CH<sub>3</sub>O), 35.0 (CH<sub>2</sub>NHCO).

**General Phosphorylation Protocol for Preparation of 3V–3Z (Description for ~3 mmol Scale).** The appropriate nucleoside **2** was coevaporated with anhydrous CH<sub>2</sub>Cl<sub>2</sub> (5 mL) and redissolved in anhydrous CH<sub>2</sub>Cl<sub>2</sub> (reagent quantities and solvent volumes are specified below). To this were added *N,N*-diisopropylethylamine (DIPEA), 0.45 M tetrazole in CH<sub>3</sub>CN, and 2-cyanoethyl-*N,N,N',N'*-tetraisopropylphosphordiamidite (PN2 reagent). The reaction mixture was stirred at rt until analytical TLC indicated complete conversion

(reaction time specified below) whereupon cold absolute EtOH (0.5 mL) was added. The reaction mixture was evaporated to dryness, and the resulting residue was purified by silica gel column chromatography (eluent specified below). The crude material was triturated from cold petroleum ether to afford phosphoramidite **3** (yields specified below).

**3'-O-(N,N-Diisopropylamino-2-cyanoethoxyphosphinyl)-5'-O-(4,4'-dimethoxytrityl)-2'-C-[4-(2,2,2-trifluoroacetamidomethyl)-1H-1,2,3-triazol-1-yl]-2'-deoxyuridine (3V).** Nucleoside **2V** (0.29 g, 0.40 mmol), DIPEA (0.10 mL, 0.57 mmol), tetrazole in CH<sub>3</sub>CN (0.45 M, 1.0 mL, 0.45 mmol), PN2 reagent (0.15 mL, 0.46 mmol), and anhydrous CH<sub>2</sub>Cl<sub>2</sub> (1 mL) were mixed, reacted (3 h), worked up, and purified (50–90% EtOAc in petroleum ether, v/v) as described above except that (a) the reaction mixture was extracted with EtOAc (5 mL) after addition of EtOH, followed by drying of the organic phase over anhydrous Na<sub>2</sub>SO<sub>4</sub> and evaporation to dryness under reduced pressure, and (b) trituration was not performed. Phosphoramidite **3V** (0.24 g, 67%) was obtained as a white solid material:  $R_f = 0.3$  (5% MeOH in CH<sub>2</sub>Cl<sub>2</sub>, v/v); MALDI-HRMS  $m/z$  945.3222 ([M + Na]<sup>+</sup>, C<sub>44</sub>H<sub>50</sub>F<sub>3</sub>N<sub>8</sub>O<sub>9</sub>·Na<sup>+</sup>, calcd 945.3283); <sup>31</sup>P NMR (CDCl<sub>3</sub>)  $\delta$  152.0, 149.8; <sup>19</sup>F NMR (CDCl<sub>3</sub>)  $\delta$  -75.7.

**3'-O-(N,N-Diisopropylamino-2-cyanoethoxyphosphinyl)-5'-O-(4,4'-dimethoxytrityl)-2'-C-[4-(pyrene-1-yl)-1H-1,2,3-triazol-1-yl]-2'-deoxyuridine (3W).** Nucleoside **2W** (230 mg, 0.29 mmol), DIPEA (0.10 mL, 0.57 mmol), tetrazole in CH<sub>3</sub>CN (0.45 M, 1.0 mL, 0.45 mmol), PN2 reagent (0.20 mL, 0.62 mmol), and anhydrous CH<sub>2</sub>Cl<sub>2</sub> (2 mL) were mixed, reacted (4 h), worked up, and purified (0–4% MeOH/CH<sub>2</sub>Cl<sub>2</sub>, v/v) as described above to afford **3W** (180 mg, 62%) as a white powder:  $R_f = 0.35$  (5% MeOH in CH<sub>2</sub>Cl<sub>2</sub>, v/v); MALDI-HRMS  $m/z$  1020.3855 ([M + Na]<sup>+</sup>, C<sub>57</sub>H<sub>56</sub>N<sub>7</sub>O<sub>8</sub>P·Na<sup>+</sup>, calcd 1020.3826); <sup>31</sup>P NMR (CDCl<sub>3</sub>)  $\delta$  152.0, 150.5.

**3'-O-(N,N-Diisopropylamino-2-cyanoethoxyphosphinyl)-5'-O-(4,4'-dimethoxytrityl)-2'-C-[4-(pyrene-1-ylcarbonyl)-1H-1,2,3-triazol-1-yl]-2'-deoxyuridine (3X).** Nucleoside **2X** (150 mg, 0.18 mmol), DIPEA (0.10 mL, 0.57 mmol), tetrazole in CH<sub>3</sub>CN (0.45 M, 0.6 mL, 0.27 mmol), PN2 reagent (0.12 mL, 0.37 mmol), and anhydrous CH<sub>2</sub>Cl<sub>2</sub> (2 mL) were mixed, reacted (3.5 h), worked up, and purified (0–4% MeOH/CH<sub>2</sub>Cl<sub>2</sub>, v/v) as described above to afford **3X** (110 mg, 59%) as a yellow solid material:  $R_f = 0.4$  (5% MeOH in CH<sub>2</sub>Cl<sub>2</sub>, v/v); MALDI-HRMS  $m/z$  1048.3779 ([M + Na]<sup>+</sup>, C<sub>58</sub>H<sub>56</sub>N<sub>7</sub>O<sub>9</sub>P·Na<sup>+</sup>, calcd 1048.3775); <sup>31</sup>P NMR (CDCl<sub>3</sub>)  $\delta$  152.4, 150.9.

**3'-O-(N,N-Diisopropylamino-2-cyanoethoxyphosphinyl)-5'-O-(4,4'-dimethoxytrityl)-2'-C-[4-(2-(pyrene-1-yl)ethyl)-1H-1,2,3-triazol-1-yl]-2'-deoxyuridine (3Y).** Nucleoside **2Y** (0.33 g, 0.40 mmol), DIPEA (0.10 mL, 0.57 mmol), tetrazole in CH<sub>3</sub>CN (0.45 M, 1.5 mL), PN2 reagent (0.25 mL, 0.78 mmol), and anhydrous CH<sub>2</sub>Cl<sub>2</sub> (2 mL) were mixed, reacted (3.5 h), worked up, and purified (0–4% MeOH/CH<sub>2</sub>Cl<sub>2</sub>, v/v) as described above to afford **3Y** (210 mg, 51%) as a white powder:  $R_f = 0.45$  (5% MeOH in CH<sub>2</sub>Cl<sub>2</sub>, v/v); MALDI-HRMS  $m/z$  1048.4147 ([M + Na]<sup>+</sup>, C<sub>59</sub>H<sub>60</sub>N<sub>7</sub>O<sub>8</sub>P·Na<sup>+</sup>, calcd 1048.4139); <sup>31</sup>P NMR (CDCl<sub>3</sub>)  $\delta$  151.6, 150.6.

**3'-O-(N,N-Diisopropylamino-2-cyanoethoxyphosphinyl)-5'-O-(4,4'-dimethoxytrityl)-2'-C-[4-(pyrene-1-yl)-carboxamidomethyl-1H-1,2,3-triazol-1-yl]-2'-deoxyuridine (3Z).** Nucleoside **2Z** (0.36 g, 0.42 mmol), DIPEA (0.10 mL, 0.57 mmol), tetrazole in CH<sub>3</sub>CN (0.45 M, 1.0 mL, 0.45 mmol), PN2 reagent (0.15 mL, 0.46 mmol), and anhydrous CH<sub>2</sub>Cl<sub>2</sub> (1 mL) were mixed, reacted (3 h), worked up, and purified (50–90% EtOAc in petroleum ether, v/v) as described above except that (a) the reaction mixture was extracted with EtOAc (5 mL) after addition of EtOH, followed by drying of the organic phase over anhydrous Na<sub>2</sub>SO<sub>4</sub> and evaporation to dryness under reduced pressure, and (b) trituration was not performed. Phosphoramidite **3Z** (0.28 g, 67%) was obtained as a white solid material:  $R_f = 0.3$  (5% MeOH in CH<sub>2</sub>Cl<sub>2</sub>, v/v); MALDI-HRMS  $m/z$  1077.3984 ([M + Na]<sup>+</sup>, C<sub>59</sub>H<sub>59</sub>N<sub>8</sub>O<sub>9</sub>P·Na<sup>+</sup>, calcd 1077.4035); <sup>31</sup>P NMR (CDCl<sub>3</sub>)  $\delta$  151.9, 150.1.

**Synthesis and Purification of ONs.** Synthesis of modified oligodeoxyribonucleotides (ONs) was performed on a DNA synthesizer using 0.2  $\mu$ mol scale succinyl-linked LCAA-CPG (long chain alkyl amine-controlled pore glass) columns with a pore size of 500 Å. Standard protocols for incorporation of DNA phosphoramidites were

used. A ~50-fold molar excess of modified phosphoramidites in anhydrous acetonitrile (at 0.05 M) was used during hand-couplings under the conditions specified in the article. Moreover, extended oxidation (45 s) was employed during hand-couplings. Cleavage from solid support and removal of protecting groups was accomplished upon treatment with 32% aqueous ammonia (55 °C, 20 h). Purification of all modified ONs was performed by ion-pair reverse-phase HPLC as described below followed by detritylation (80% aqueous AcOH) and precipitation from acetone (-18 °C for 12–16 h).

Purification of crude ONs was performed on a HPLC system equipped with an XTerra MS C18 precolumn (10  $\mu$ m, 7.8 × 10 mm) and an XTerra MS C18 column (10  $\mu$ m, 7.8 × 150 mm) using a 0.05 mM TEAA (triethylammonium acetate) buffer: 25% water/acetonitrile (v/v) gradient. The identity of synthesized ONs was established through analysis on a quadrupole time-of-flight tandem mass spectrometer equipped with a MALDI source (positive ion mode) using anthranilic acid as a matrix (Table S1 in Supporting Information), while purity (>80%) was verified by ion-pair reverse-phase HPLC running in analytical mode.

**Thermal Denaturation Studies.** Concentrations of ONs were estimated using the following extinction coefficients (OD/ $\mu$ mol): dG (12.01), dA (15.20), dT (8.40), dC (7.05); rG (13.70), rA (15.40), rU (10.00), rC (9.00); V (19.96), W (31.08), X (35.60), Y (27.62) and Z (30.95) [values for monomers V–Z were estimated through  $A_{260}$  measurements of the corresponding phosphoramidites in 1% aqueous DMSO solutions]. Each strand was thoroughly mixed and denatured by heating to 80–85 °C followed by cooling to the starting temperature of the experiment. Quartz optical cells with a path length of 10 mm were used. Thermal denaturation temperatures ( $T_m$  values [°C]) of duplexes (1.0  $\mu$ M final concentration of each strand) were measured on a UV/vis spectrophotometer equipped with a 12-cell Peltier temperature controller and determined as the maximum of the first derivative of the thermal denaturation curve ( $A_{260}$  vs  $T$ ) recorded in medium salt buffer ( $T_m$  buffer: 100 mM NaCl, 0.1 mM EDTA, and pH 7.0 adjusted with 10 mM Na<sub>2</sub>HPO<sub>4</sub> and 5 mM Na<sub>2</sub>HPO<sub>4</sub>). The temperature of the denaturation experiments ranged from at least 20 °C below  $T_m$  to 20 °C above  $T_m$ . A temperature ramp of 0.5 °C/min was used in all experiments. Reported  $T_m$  values are averages of two experiments within  $\pm 1.0$  °C.

**Steady-State Fluorescence Emission Spectra.** Spectra of ONs modified with pyrene-functionalized monomers W/X/Y/Z and the corresponding duplexes with complementary or mismatched DNA/RNA targets were recorded in nondeoxygenated thermal denaturation buffer (each strand 1.0  $\mu$ M) using an excitation wavelength of  $\lambda_{ex} = 350$  nm for W/Y/Z or  $\lambda_{ex} = 400$  nm for X, excitation slit 5.0 nm, emission slit 5.0 nm, and a scan speed of 600 nm/min. Experiments were performed at ambient temperature (~20 °C).

**Determination of Quantum Yields.** Relative fluorescence emission quantum yields ( $\Phi_F$ ) of modified nucleic acids (SSP or duplex) were determined using the following equation:<sup>61</sup>

$$\Phi_F(\text{NA}) = \frac{[\Phi_F(\text{std})/\alpha(\text{std})] \times [\text{IFI}(\text{NA})/A_{ex}(\text{NA})] \times [n(\text{NA})/n(\text{std})]^2}{[\Phi_F(\text{std})/\alpha(\text{std})] \times [\text{IFI}(\text{NA})/A_{ex}(\text{NA})] \times [n(\text{NA})/n(\text{std})]^2}$$

where  $\Phi_F(\text{std})$  is the fluorescence emission quantum yield of the standard;  $\alpha(\text{std})$  is the slope of the integrated fluorescence intensity versus optical intensity plot made for the standard; IFI(NA) is the integrated fluorescence intensity ( $\lambda_{em} = 360$ –510 nm for monomer W/Y/Z;  $\lambda_{em} = 425$ –625 nm for monomer X;  $\lambda_{em} = 360$ –600 nm for standards);  $A_{ex}(\text{NA})$  is the optical density of the sample at the utilized excitation wavelength ( $\lambda_{ex} = 350$  nm for monomer W/X/Z;  $\lambda_{ex} = 400$  nm for monomer X;  $\lambda_{ex} = 350$  nm for standards; optical densities of all solutions at the excitation wavelengths were between 0.01 and 0.10);  $n(\text{NA})$  and  $n(\text{std})$  are refractive indexes of solvents used for sample and standard, respectively ( $n_{\text{water}} = 1.33$ ,  $n_{\text{ethanol}} = 1.36$ , and  $n_{\text{cyclohexane}} = 1.43$ ).

The validity of this method under our experimental setup was ascertained by determining the quantum yield of anthracene in ethanol with respect to 9,10-diphenylanthracene in cyclohexane ( $\Phi_F = 0.86$ ).<sup>61</sup> The measured value of  $\Phi_F = 0.28$  is in excellent agreement with the



reported value of ( $\Phi_F = 0.27$ ).<sup>62</sup> Subsequently, the literature value for anthracene in ethanol was used as the standard for determination of quantum yields of SSPs and duplexes.

## ■ ASSOCIATED CONTENT

### ● Supporting Information

NMR spectra of all new compounds; MS data of modified ONs; representative thermal denaturation profiles;  $T_m$  values for 9-mer ONs modified with monomers V and Z; additional thermal denaturation, fluorescence and absorbance data for duplexes with matched/mismatched RNA targets. This material is available free of charge via the Internet at <http://pubs.acs.org>.

## ■ AUTHOR INFORMATION

### Corresponding Author

\*E-mail: [hrdlicka@uidaho.edu](mailto:hrdlicka@uidaho.edu).

## ■ ACKNOWLEDGMENTS

We appreciate support from Award Number R01 GM088697 from the National Institute of General Medical Sciences, National Institutes of Health. We thank Dr. Lee Deobald, Prof. Andrzej J. Paszczyński (both EBI Murdock Mass Spectrometry Center, Univ. Idaho), Prof. Matthew J. Morra, and Dr. Vladimir Borek (both Division of Soil & Land Resources, Univ. Idaho) for mass spectrometric analyses. The assistance of Dr. Andreas S. Madsen (Technical University of Denmark) and Dr. Jakob Magolan (University of Idaho) during preparation of the cover illustration is greatly appreciated.

## ■ REFERENCES

- (1) Rostovtsev, V. V.; Green, L. G.; Fokin, V. V.; Sharpless, K. B. *Angew. Chem., Int. Ed.* **2002**, *41*, 2596–2599.
- (2) Tornøe, C. W.; Christensen, C.; Meldal, M. *J. Org. Chem.* **2002**, *67*, 3057–3064.
- (3) Amblard, F.; Cho, J. H.; Schinazi, R. F. *Chem. Rev.* **2009**, *109*, 4207–4220.
- (4) Ustinov, A. V.; Stepanova, I. A.; Dubnyakova, V. V.; Zatsepin, T. S.; Nozhevnikova, E. V.; Korshun, V. A. *Russ. J. Bioorg. Chem.* **2010**, *36*, 437–481.
- (5) El-Sagheer, A. H.; Brown, T. *Chem. Soc. Rev.* **2010**, *39*, 1388–1405.
- (6) (a) Seo, T. S.; Li, Z.; Ruparel, H.; Ju, J. *J. Org. Chem.* **2003**, *68*, 609–612. (b) Gierlich, J.; Burlley, G. A.; Gramlich, P. M. E.; Hammond, D. M.; Carell, T. *Org. Lett.* **2006**, *8*, 3339–3342. (c) Seela, F.; Sirivolu, V. R.; Chittepu, P. *Bioconjugate Chem.* **2008**, *19*, 211–224. (d) Seela, F.; Ming, X. *Helv. Chim. Acta* **2008**, *91*, 1181–1200. (e) Berndl, S.; Herzig, N.; Kele, P.; Lachmann, D.; Li, X.; Wolfbeis, O. S.; Wagenknecht, H.-A. *Bioconjugate Chem.* **2009**, *20*, 558–564. (f) Seela, F.; Ingale, S. A. *J. Org. Chem.* **2010**, *75*, 284–295. (g) Ding, P.; Wunnicke, D.; Steinhoff, H.-J.; Seela, F. *Chem.—Eur. J.* **2010**, *16*, 14385–14396. (h) Jakobsen, U.; Shelke, S. A.; Vogel, S.; Sigurdsson, S. T. *J. Am. Chem. Soc.* **2010**, *132*, 10424–10428. (i) Onizuka, K.; Shibata, A.; Taniguchi, Y.; Sasaki, S. *Chem. Commun.* **2011**, *47*, 5004–5006. (j) Kuboyama, T.; Nakahara, M.; Yoshino, M.; Cui, Y.; Sako, T.; Wada, Y.; Imanishi, T.; Obika, S.; Watanabe, Y.; Suzuki, M.; Doi, H. *Bioorg. Med. Chem.* **2011**, *19*, 249–255. (k) Mercier, F.; Paris, J.; Kaisin, G.; Thonon, D.; Flagthier, J.; Teller, N.; Lemaire, C.; Luxen, A. *Bioconjugate Chem.* **2011**, *22*, 108–114.
- (7) Burlley, G. A.; Gierlich, J.; Mofid, M. R.; Nir, H.; Tal, S.; Eichen, Y.; Carell, T. *J. Am. Chem. Soc.* **2006**, *128*, 1398–1399.
- (8) Kumar, R.; El-Sagheer, A.; Tumpane, J.; Lincoln, P.; Wilhelmsson, L. M.; Brown, T. *J. Am. Chem. Soc.* **2007**, *129*, 6859–6864.
- (9) Xiong, H.; Seela, F. *J. Org. Chem.* **2011**, *76*, 5584–5597.
- (10) (a) Isobe, H.; Fujino, T.; Yamazaki, N.; Guillot-Nieckowski, M.; Nakamura, E. *Org. Lett.* **2008**, *10*, 3729–3732. (b) Mutisya, D.; Selvam, C.; Kennedy, S. D.; Rozners, E. *Bioorg. Med. Chem. Lett.* **2011**, *21*, 3420–3422. (c) El-Sagheer, A. H.; Brown, T. *Proc. Natl. Acad. Sci. U.S.A.* **2010**, *107*, 15329–15334.
- (11) Chittepu, P.; Sirivolu, V. R.; Seela, F. *Bioorg. Med. Chem.* **2008**, *16*, 8427–8439.
- (12) Nakahara, M.; Kuboyama, T.; Izawa, A.; Hari, Y.; Imanishi, T.; Obika, S. *Bioorg. Med. Chem. Lett.* **2009**, *19*, 3316–3319.
- (13) Østergaard, M. E.; Guenther, D. C.; Kumar, P.; Baral, B.; Deobald, L.; Paszczyński, A. J.; Sharma, P. K.; Hrdlicka, P. J. *Chem. Commun.* **2010**, *46*, 4929–4931.
- (14) Kumar, T. S.; Wengel, J.; Hrdlicka, P. J. *ChemBioChem* **2007**, *8*, 1122–1125.
- (15) Østergaard, M. E.; Kumar, P.; Baral, B.; Guenther, D. C.; Anderson, B. A.; Ytreberg, F. M.; Deobald, L.; Paszczyński, A. J.; Sharma, P. K.; Hrdlicka, P. J. *Chem.—Eur. J.* **2011**, *17*, 3157–3165.
- (16) Østergaard, M. E.; Hrdlicka, P. J. *Chem. Soc. Rev.* **2011**, DOI: 10.1039/C1CS15014F.
- (17) Østergaard, M. E.; Cheguru, P.; Papasani, M. R.; Hill, R. A.; Hrdlicka, P. J. *J. Am. Chem. Soc.* **2010**, *132*, 14221–14228.
- (18) Kumar, T. S.; Madsen, A. S.; Østergaard, M. E.; Wengel, J.; Hrdlicka, P. J. *J. Org. Chem.* **2008**, *73*, 7060–7066.
- (19) Kumar, T. S.; Madsen, A. S.; Østergaard, M. E.; Sau, S. P.; Wengel, J.; Hrdlicka, P. J. *J. Org. Chem.* **2009**, *74*, 1070–1081.
- (20) Sau, S. P.; Kumar, T. S.; Hrdlicka, P. J. *Org. Biomol. Chem.* **2010**, *8*, 2028–2036.
- (21) Karmakar, S.; Anderson, B. A.; Rathje, R. L.; Andersen, S.; Jensen, T.; Nielsen, P.; Hrdlicka, P. J. *J. Org. Chem.* **2011**, *76*, 7119–7131.
- (22) Yamana, K.; Iwase, R.; Furutani, S.; Tsuchida, H.; Zako, H.; Yamaoka, T.; Murakami, A. *Nucleic Acids Res.* **1999**, *27*, 2387–2392.
- (23) Nakamura, M.; Fukunaga, Y.; Sasa, K.; Ohtoshi, Y.; Kanaori, K.; Hayashi, H.; Nakano, H.; Yamana, K. *Nucleic Acids Res.* **2005**, *33*, 5887–5895.
- (24) Kalra, N.; Babu, B. R.; Parmar, V. S.; Wengel, J. *Org. Biomol. Chem.* **2004**, *2*, 2885–2887.
- (25) Jawalekar, A. M.; Meeuwenoord, N.; Cremers, J. S. G. O.; Overkleef, H. S.; Marel, G. A. V. D.; Rutjes, F. P. J. T.; Delft, F. L. V. *J. Org. Chem.* **2008**, *73*, 287–290.
- (26) Jørgensen, A. S.; Shaikh, K. I.; Enderlin, G.; Ivarsen, E.; Kumar, S.; Nielsen, P. *Org. Biomol. Chem.* **2011**, *9*, 1381–1388.
- (27) Kiviniemi, A.; Virta, P.; Drenichev, M. S.; Mikhailov, S. N.; Lönnberg, H. *Bioconjugate Chem.* **2011**, *22*, 1249–1255.
- (28) Patil, R. V.; Dekker, E. E. *Nucleic Acids Res.* **1990**, *18*, 3080–3080.
- (29) Nichols, R.; Andrews, P. C.; Zhang, P.; Bergstrom, D. E. *Nature* **1994**, *369*, 492–493.
- (30) Loakes, D.; Brown, D. M.; Linde, S.; Hill, F. *Nucleic Acids Res.* **1995**, *23*, 2361–2366.
- (31) Chizhikov, V.; Wagner, M.; Ivshina, A.; Hoshino, Y.; Kapikian, A. Z.; Chumakov, K. J. *Clin. Microbiol.* **2002**, *40*, 2398–2407.
- (32) Too, K.; Loakes, D. Universal Base Analogues and their Application to Biotechnology. In *Modified Nucleosides: In Biochemistry, Biotechnology and Medicine*, Herdewijn, P., Ed.; Wiley-VCH: Weinheim, Germany, 2008; pp 277–303.
- (33) Loakes, D.; Brown, D. M. *Nucleic Acids Res.* **1994**, *22*, 4039–4043.
- (34) Berger, M.; Wu, Y.; Ogawa, A. K.; McMinn, D. L.; Schultz, P. G.; Romesberg, F. E. *Nucleic Acids Res.* **2000**, *28*, 2911–2914.
- (35) Matray, T. J.; Kool, E. T. *J. Am. Chem. Soc.* **1998**, *120*, 6191–6192.
- (36) Babu, B. R.; Wengel, J. *Chem. Commun.* **2001**, 2114–2115.
- (37) Raunak; Babu, B. R.; Parmar, V. S.; Harrit, N. H.; Wengel, J. *Org. Biomol. Chem.* **2004**, *2*, 80–89.
- (38) MacKinnon, K. F.; Qualley, D. F.; Woski, S. A. *Tetrahedron Lett.* **2007**, *48*, 8074–8077.
- (39) Seela, F.; Chen, Y. *Nucleic Acids Res.* **1995**, *23*, 2499–2505.
- (40) Acedo, M.; De Clercq, E.; Eritja, R. *J. Org. Chem.* **1995**, *60*, 6262–6269.

- (41) Cubero, E.; Güimil-García, R.; Luque, F. J.; Eritja, R.; Orozco, M. *Nucleic Acids Res.* **2001**, *29*, 2522–2534.
- (42) Seela, F.; Debelak, H. *Nucleic Acids Res.* **2000**, *28*, 3224–3232.
- (43) Koller, A. N.; Bozilovic, J.; Engels, J. W.; Gohlke, H. *Nucleic Acids Res.* **2010**, *38*, 3133–3146.
- (44) For a successful example, see: Köhler, O.; Jarikote, D. V.; Seitz, O. *ChemBioChem* **2005**, *6*, 69–77.
- (45) Patra, A.; Richert, C. *J. Am. Chem. Soc.* **2009**, *131*, 12671–12681.
- (46) Trybulski, E. J.; Zhang, J.; Kramss, R. H.; Mangano, R. M. *J. Med. Chem.* **1993**, *36*, 3533–3541.
- (47) Liu, F.; Tang, C.; Chen, Q.-Q.; Li, S.-Z.; Wu, H.-B.; Xie, L.-H.; Peng, B.; Wei, W.; Cao, Y.; Huang, W. *Org. Electron.* **2009**, *10*, 256–265.
- (48) Okamoto, A.; Kanatani, K.; Saito, I. *J. Am. Chem. Soc.* **2004**, *126*, 4820–4827.
- (49) Sanghvi, Y. S.; Hoke, G. D.; Freier, S. M.; Zounes, M. C.; Gonzalez, C.; Cummins, L.; Sasmor, H.; Cook, P. D. *Nucleic Acids Res.* **1993**, *21*, 3197–3203.
- (50) Oliver, J. S.; Parker, K. A.; Suggs, J. W. *Org. Lett.* **2001**, *3*, 1977–1980.
- (51) Millican, T. A.; Mock, G. A.; Chauncey, M. A.; Patel, T. P.; Eaton, M. A. W.; Gunning, J.; Cutbush, S. D.; Neidle, S.; Mann, J. *Nucleic Acids Res.* **1984**, *12*, 7435–7453.
- (52) Langenegger, S. M.; Häner, R. *ChemBioChem* **2005**, *6*, 848–851.
- (53) Nakano, S.; Uotani, Y.; Uenishi, K.; Fujii, M.; Sugimoto, N. *Nucleic Acids Res.* **2005**, *33*, 7111–7119.
- (54) Verhagen, C.; Bryld, T.; Raunkjær, M.; Vogel, S.; Buchalová, K.; Wengel, J. *Eur. J. Org. Chem.* **2006**, 2538–2548.
- (55) Dougherty, G.; Pilbrow, J. R. *Int. J. Biochem.* **1984**, *16*, 1179–1192.
- (56) Manoharan, M.; Tivel, K. L.; Zhao, M.; Nafisi, K.; Netzel, T. L. *J. Phys. Chem.* **1995**, *99*, 17461–1747.
- (57) Seo, Y. J.; Ryu, J. H.; Kim, B. H. *Org. Lett.* **2005**, *7*, 4931–4933.
- (58) Jiang, Y. L.; Kwon, K.; Stivers, J. T. *J. Biol. Chem.* **2001**, *276*, 42347–42354.
- (59) Beuck, C.; Singh, I.; Bhattacharya, A.; Hecker, W.; Parmar, V. S.; Seitz, O.; Weinhold, E. *Angew. Chem., Int. Ed.* **2003**, *42*, 3958–3960.
- (60) Fleming, D. A.; Thode, C. J.; Williams, M. E. *Chem. Mater.* **2006**, *18*, 2327–2334.
- (61) Morris, J. V.; Mahaney, M. A.; Huber, J. R. *J. Phys. Chem.* **1976**, *80*, 969–974.
- (62) Melhuish, W. H. *J. Phys. Chem.* **1961**, *65*, 229–235.